Analyst

PAPER

View Article Online
View Journal

A compact QCL based methane and nitrous oxide sensor for environmental and medical applications

Cite this: DOI: 10.1039/c3an01452e

Mohammad Jahjah,[a] Wei Ren,[a] Przemysław Stefański,[a] Rafał Lewicki,[a] Jiawei Zhang,[ac] Wenzhe Jiang,[a] Jan Tarka[ab] and Frank K. Tittel*[a]

Received 30th July 2013
Accepted 7th January 2014

DOI: 10.1039/c3an01452e

www.rsc.org/analyst

A methane (CH_4) and nitrous oxide (N_2O) sensor based on a sensitive, selective and well established technique of quartz enhanced photoacoustic spectroscopy (QEPAS) was developed for environmental and biomedical measurements. A thermoelectrically cooled (TEC) distributed feedback quantum cascade laser (DFB-QCL), capable of continuous wave (CW) mode hop free emission in the 7.83 μm wavelength range, was used as an excitation source. For the targeted CH_4 and N_2O absorption lines located at 1275.04 cm^{-1} and 1275.49 cm^{-1} detection limits (1σ) of 13 ppbv and 6 ppbv were achieved with a 1 second data acquisition time, respectively. Environmental data of CH_4 and N_2O mixing ratios acquired using the QEPAS sensor system are also reported.

Introduction

CH_4 and N_2O next to CO_2 are the most important greenhouse gases because of their global warming potential.[1–3] Therefore, the detection of CH_4 and N_2O at low parts per billion (ppb) concentration levels is of great interest in environmental[4,5] and agricultural monitoring.[6] Furthermore, exposure to N_2O can lead to a short-term decrease in mental performance, audio-visual ability, and manual dexterity.[7] N_2O is also a processing gas in electronics[8] as well as in medicine[9,10] and in aerospace applications.[11,12]

Several optical sensing techniques have been employed to achieve quantitative and selective detection of atmospheric trace gases. Recently, a quantum cascade laser (QCL) based CH_4 and N_2O sensor system capable of a detection limit of 7 ppbv and 2 ppbv, respectively when using a 215 m pathlength multi-pass gas cell was reported.[13] Ambient CH_4 and N_2O monitoring was also performed using a mid-IR difference frequency generation (DFG) laser system combined with a 5 m long Herriott cell.[14] An averaging time of 10 s is required to achieve ppb-level detection. However, such a sensor system is complex due to the DFG laser configuration which requires two diode lasers and fiber amplifiers. Cavity enhanced absorption spectroscopy (CEAS) based N_2O detection achieved a detection limit of 10 ppbv when targeting a N_2O absorption line at 4.530 μm.[15] In this technique, two pairs of mirrors with high-reflectivity (>99.9%) as well as critical optical alignments were required to achieve optimal performance of the CEAS based sensor system. Photoacoustic detection of N_2O was recently reported using an 8 μm QCL and reached a detection limit of 80–100 ppbv, which is not sufficient for environmental monitoring.[16]

In this work, a quartz-enhanced photoacoustic absorption spectroscopy (QEPAS) technique is used for trace gas detection, invented in 2002 at Rice University.[17,18] QEPAS uses a quartz tuning fork (QTF) as a sharply resonant acoustic transducer with a high Q factor (typically $>10^4$) in an innovative way. The QTF converts the acoustic wave created by gas absorption of a laser beam, typically modulated at half of the QTF resonance frequency, into an electrical signal due to its piezoelectric properties. The amplitude of the detected signal is proportional to the absorption coefficient, concentration of a targeted gas, and the QCL excitation power.[19] QEPAS employs commercially available QTFs that have resonant frequency (f_0) of 32.768 kHz and a high Q factor of $\sim 10^4$ at atmospheric pressure. QEPAS possesses high immunity to environmental acoustic noise due to the fact that acoustically a QTF is a quadrupole, in which case only the anti-symmetric vibration of a QTF is piezo-electrically active. Moreover, the dimensions of the QTF are small (~ 2 mm^3),[20] which results in an ultra-compact gas cell and a fast gas exchange.[21] The QEPAS sensor uses a 7.83 μm CW TEC DFB-QCL as an excitation source. The available laser wavelength tuning range is suitable for simultaneous monitoring of absorption lines of CH_4 and N_2O molecules. Characterization of the DFB-QCL based QEPAS sensor platform includes a determination of the minimum detection limit using a commercially calibrated gas mixture. Furthermore, the linear response and long term stability of the sensor system are discussed.

[a]Rice University, Department of Electrical and Computer Engineering, 6100 Main Street, Houston, TX 77005, USA. E-mail: fkt@rice.edu

[b]Laser & Fiber Electronics Group, Wroclaw University of Technology, Wybrzeze Wyspianskiego 27, Wroclaw, 50-370, Poland

[c]Northeast Forestry University, School of Electromechanical Engineering, Harbin, 150040, Heilongjiang Province, China

Characterization of a 7.83 μm CW TEC DFB-QCL

Mid-infrared QCLs[22] are used as convenient compact spectroscopic sources in laser based sensor systems for sensitive, selective and precise trace gas monitoring in a variety of applications[23] including environmental applications[24–26] and medical diagnostics.[10] A 7.83 μm CW DFB-QCL (AdTech Optics, Part no. HHL-12-25) enclosed in a high heat load (HHL) package was used as the excitation source. An aspheric lens is placed directly in front of the DFB-QCL in order to collimate the emitted beam. The HHL package is sealed by a ZnSe window that transmits ~95% of the QCL output power. The QCL power as well as the current and temperature tuning curves were determined by using an optical power meter and a Fourier transform infrared (FTIR) spectrometer, respectively. Fig. 1(a) and (b) show the DFB-QCL characteristics at different operating temperatures. From the experimental results depicted in Fig. 1(b), the DFB-QCL current and temperature tuning coefficients were determined to be $-0.01\ cm^{-1}\ mA^{-1}$ and $-0.11\ cm^{-1}\ °C^{-1}$, respectively.

QEPAS sensor platform

The CH_4 and N_2O QEPAS based sensor architecture, depicted in Fig. 2, consists of a 7.83 μm CW TEC DFB-QCL, a spatial filter consisting of 200 μm pinhole as well as a germanium (f = 40 mm) and zinc selenide (f = 25 mm) plano-convex lenses for beam enhancement and focusing, and an acoustic detection module (ADM) that includes a QTF, an acoustic micro-resonator (mR)[27] and a low noise preamplifier. By introducing a spatial filter into the sensor system the QCL beam quality was significantly improved at the expense of ~30% loss of QCL output power. The acoustic mR consists of two hypodermic tubes, which are 4.4 mm in length and have an inner diameter of 0.6 mm. Each tube was mounted on one side of the QTF at a distance of ~40 μm from its surface. The selected mR tube dimensions resulted in an increased signal-to-noise ratio of the detected photoacoustic signal and improved the optical power transmission through the mR and the QTF to ~99%. The QTF and mR were enclosed inside a compact, stainless steel gas cell that uses anti-reflection coated zinc selenide windows. The entire optical system was mounted on a platform with dimensions of 30 cm × 15 cm × 15 cm.

The DFB-QCL is driven by a laser current source (ILX, model LDX-3232), and its temperature is regulated by a temperature controller (Wavelength electronics, LFI, model 3751). A custom built control electronics unit (CEU) is used to determine the parameters of the QTF (resistance R, Q-factor and resonant frequency: f_0), to modulate the QCL emitted light at half of the QTF resonant frequency ($f_m = f_0/2$), as well as to measure both the $2f$ and the $3f$ components generated by the QTF with an external reference cell and a photodetector, respectively. Second harmonic ($2f$) detection was implemented in order to improve

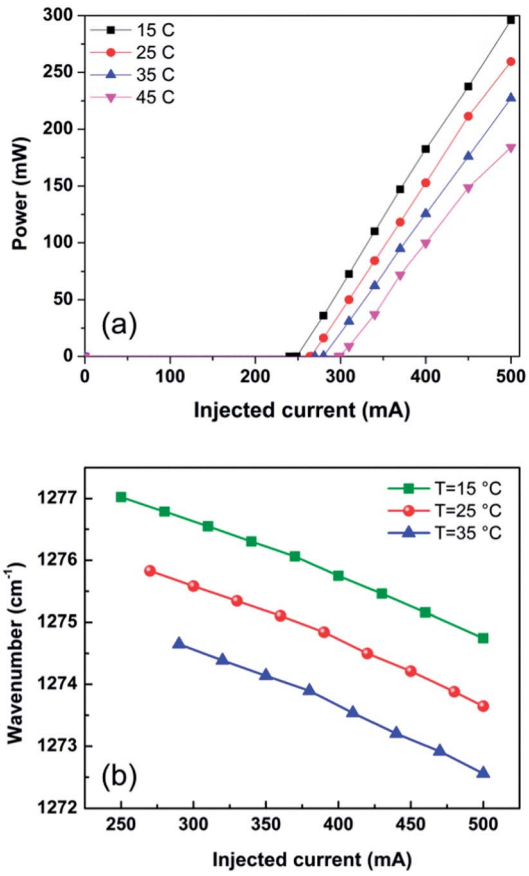

Fig. 1 (a) Light intensity (LI) curves of a 7.83 μm CW DFB-QCL (AdTech Optics); (b) DFB-QCL emitted wavelengths as a function of injected current at three operating temperatures 15 °C, 25 °C and 35 °C.

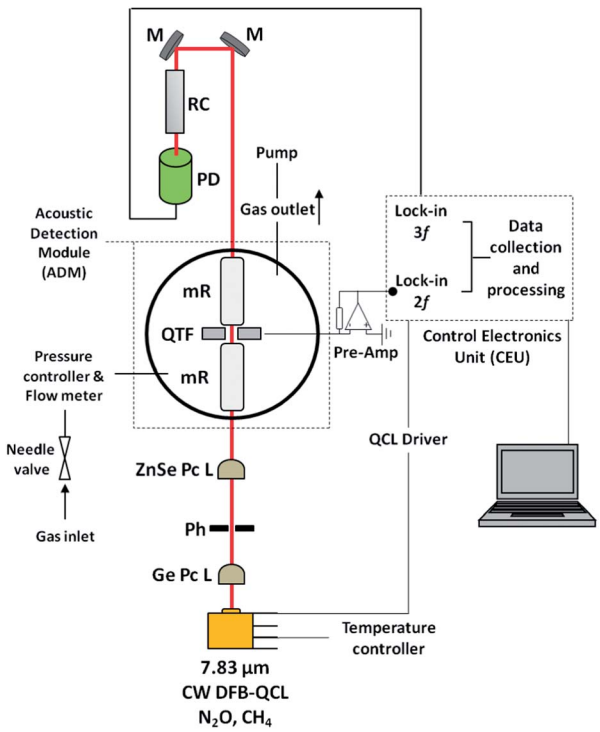

Fig. 2 Schematic of CH_4 and N_2O QEPAS sensor. Ge Pc L and ZnSe Pc L – plano-convex lenses, Ph – pinhole, M – mirror, QTF – quartz tuning fork, mR – acoustic micro-resonator, RC – reference cell, PD – pyroelectric-detector.

the sensitivity of the QEPAS sensor and the 3*f* signal assured locking the targeted absorption line to the DFB-QCL frequency. The CEU which contains the electronics necessary to acquire and process the QEPAS data has dimensions of 25 cm × 25 cm × 10 cm.

The interaction of an acoustic wave with the electrodes of the QTF prongs, results in a charge transfer to the QTF due to its piezoelectric properties. The current signal is then amplified and converted into a voltage by means of an ultra-low noise transimpedance amplifier with a 10 MΩ feedback resistor. The 2*f* harmonic data is collected with LabView-based software installed on a laptop connected with the CEU *via* a serial port. A pressure controller (MKS Instruments, Type 640) and a vacuum pump were connected to the gas outlet of the ADM, in order to control and maintain the CH_4 and N_2O sensor system pressure at a constant level of 130 Torr. After passing through the ADM, the DFB-QCL beam is collected by a pyroelectric-detector placed after a 5 cm long reference cell (Wavelength reference, Inc). The reference cell filled with a calibrated concentration of 0.5% of CH_4 and 1% of N_2O at 100 Torr was used for line-locking measurements.

CH_4 and N_2O detection

The high resolution transmission (HITRAN) absorption database[28] was used to simulate absorption spectra accessible in the emitted wavelength range of the available CW TEC DFB-QCL. Fig. 3 shows the gas absorption spectra within the laser tuning range for a mixture of 1.8 ppmv of CH_4, 320 ppbv of N_2O, 400 ppbv of CO_2 and 2% of H_2O at 130 Torr and for an optical pathlength of 1 m.

For sensitive and accurate QEPAS measurements interference free CH_4 and N_2O rotational-vibrational absorption lines located at 1275.04 cm^{-1} and 1275.49 cm^{-1} were targeted respectively. The detection of CH_4 and N_2O absorption lines was realized by stabilizing the temperature of the 7.83 μm DFB-QCL at 21.5 °C and linearly tuning its injected current from 430 to 500 mA.

Four different measurements were realized, starting with determining the QEPAS sensor baseline by acquiring a complete scan when the ADM was filled with pure N_2, subsequently detecting the targeted molecules in ambient air, and finishing by using calibrated gas mixtures of 1 ppmv and 1.8 ppmv of CH_4 and N_2O, respectively. CH_4 and N_2O mixing ratios were detected with an output power from the DFB-QCL that exceeds 120 mW inside the ADM and their 2*f* signals are presented in Fig. 4.

The QEPAS signal amplitude for a slowly relaxing molecule such as CH_4 or N_2O is dependent on the vibrational–translational (V–T) relaxation rate. Hence the addition of water vapor to the analyzed gas mixture helps to efficiently improve the V–T process, thus enhancing the 2*f* QEPAS signal. In this work, a commercial permeation tube (Perma Pure model MH-110-24F-4), which was immersed inside a water circulating bath (LAUDA-Brinkmann, LP., RM6), was utilized to maintain the water concentration in the analyzed gas mixture and thus constantly enhance the QEPAS signal amplitude by a factor of 3. Further discussion of this technique can be found in ref. 29–32.

The pressure inside the ADM was set to 130 Torr. For such conditions, the QTF resonant frequency was determined by the CEU to be 32 767 Hz and the modulation frequency was automatically set to 16 383.5 Hz for 2f detection. Based on the two measurements shown in Fig 4, for the N_2O absorption line located at 1275.49 cm^{-1}, the N_2O ambient laboratory concentration was calculated to be 331 ppbv. The minimum detectable concentration (MDC) for CH_4 (1275.04 cm^{-1}) and N_2O (1275.49 cm^{-1}) molecules was determined to be 13 ppbv and 6 ppbv, respectively for a 1 second averaging time and at 1σ.

The linear response of the QEPAS sensor, depicted in Fig. 5 was investigated, by plotting the lock-in amplifier output signal as a function of the CH_4 calibrated concentration in the ADM (*i.e.* 1000, 500, 250, 125 and 62.5 ppbv).

The DFB-QCL injected current was varied between 487 mA and 497 mA maintained at an operating temperature of 21.5 °C. The gas dilution was performed by using a commercial gas mixing system (Environics Inc, "series 4040"). These measurements were

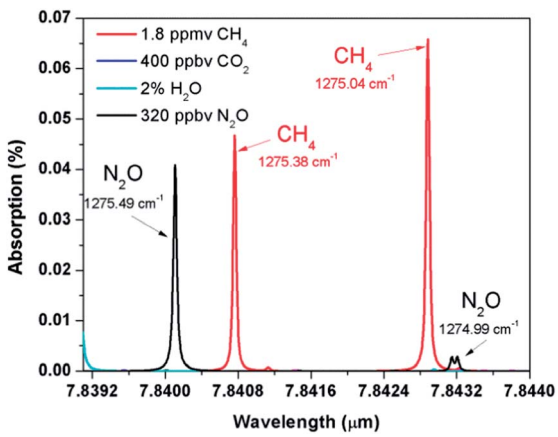

Fig. 3 HITRAN simulation of CH_4 and N_2O absorption spectra in the 7.83 μm wavelength range ($P = 130$ Torr, $L = 1$ m). Atmospheric H_2O and CO_2 have negligible absorption within this wavelength range.

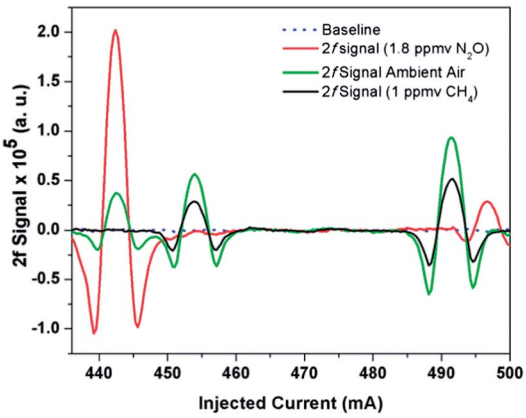

Fig. 4 2*f* QEPAS signals of CH_4 and N_2O: in ambient air (green curve), from a moisturized 1.8 ppmv mixture of N_2O in N_2 (red curve) and 1 ppmv of CH_4 in N_2 (black curve). The QEPAS sensor baseline is represented by a dotted blue curve. Total gas pressure for the four spectral scans was $P = 130$ Torr.

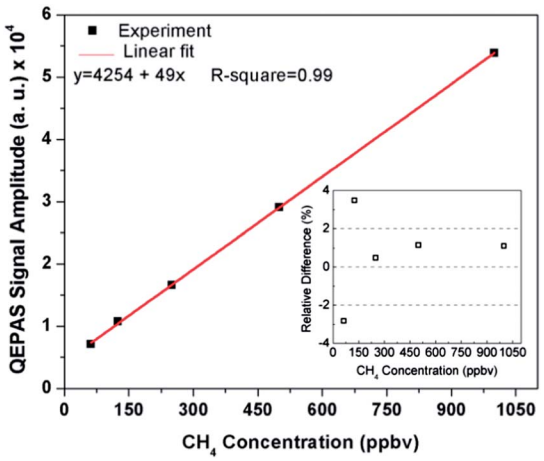

Fig. 5 QEPAS signal amplitude as function of the CH_4 concentration. Inset: relative difference between measurement results and linear fit values.

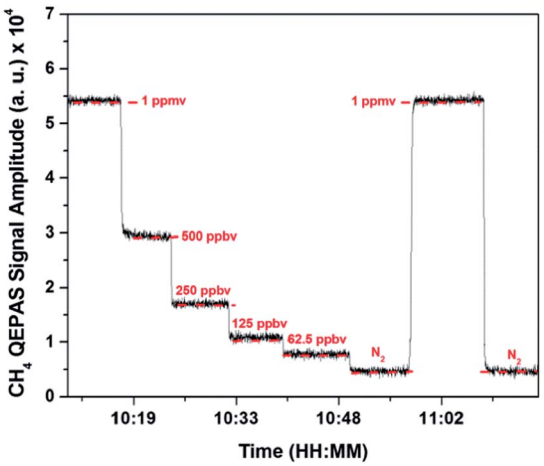

Fig. 6 Continuous monitoring of CH_4 calibrated concentrations. Solid line, measurement; dashed line, calibrated CH_4 concentration.

realized using a 3*f* reference channel and locking the DFB-QCL frequency to the peak of the CH_4 absorption line located at 1275.04 cm^{-1} ($T = 21.5$ °C; $I = 492$ mA). A feedback loop is used to eliminate any laser frequency drift caused by DFB-QCL current or/and temperature variations. The linear response of the QEPAS signal amplitude for different CH_4 concentration values is depicted in Fig 5, along with the relative difference between measurements and linear fit values shown in the inset graph of Fig 5. The *R*-square value for linear fitting is >0.99 and the relative difference between the measured and the calculated CH_4 concentration based on the determined linear equation is within 4% (actually <2% when CH_4 concentration is higher than 125 ppb).

The stability of the QEPAS sensor was studied by monitoring continuously different CH_4 concentrations during 1 h while operating the sensor in the 3*f* line-locking mode. The measurements (solid line) and calibrated CH_4 concentrations (dashed line) are presented in Fig 6. The CH_4 QEPAS signal amplitude remains stable for different CH_4 mixing ratios. The

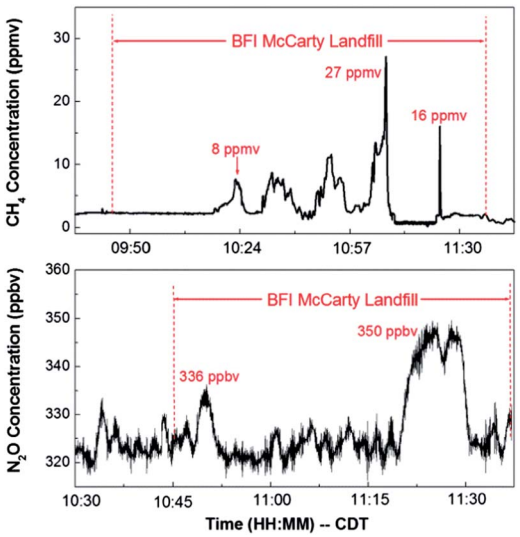

Fig. 7 CH_4 and N_2O mixing ratios measured using QEPAS sensor system near the BFI McCarty landfill, TX, on September 10th and 26th 2013, respectively.

QEPAS sensor reproducibility was tested after 45 minutes of continuous measurements by detecting 1 ppmv of CH_4. These measurements indicate both the stability and robustness of the reported DFB-QCL based QEPAS sensor system.

Furthermore, atmospheric CH_4 and N_2O mixing ratios were measured at the BFI McCarty landfill, an urban solid waste disposal site in the Greater Houston area with the QEPAS sensor system. For these field measurements the QEPAS based sensor system was installed in the Aerodyne Research, Inc. mobile laboratory (AML) during the September 2013 Houston-based NASA field campaign *DISCOVER-AQ* (Deriving Information on Surface Conditions from Column and Vertically Resolved Observations Relevant to Air Quality). Representative measurements of CH_4 and N_2O mixing ratios were plotted in Fig. 7 as the AML circled the BFI McCarty landfill. Good agreement was found (within a 5% difference) between measurements recorded by both the QEPAS sensor and the AML van based CH_4 DFB-QCL multi-pass absorption cell gas sensor systems.

Conclusions and outlook

This study described a 7.83 μm CW TEC DFB-QCL QEPAS sensor platform employing 2*f* detection for sensitive measurements of CH_4 and N_2O concentration levels. Minimum detectable concentration levels (1σ) for CH_4 and N_2O are 13 ppbv and 6 ppbv, respectively with a 1 s averaging time. The linearity and the stability of the QEPAS sensor were verified by monitoring continuously different calibrated concentrations of CH_4. Atmospheric CH_4 and N_2O mixing ratios were measured at the BFI McCarty landfill, an urban solid waste disposal site in the Greater Houston area. The main advantage of the reported CH_4 and N_2O QEPAS sensor is its compact size where the total dimensions of the employed QCL, ADM and photodetector that compose the reported trace-gas sensor fulfil the requirements of a small *in situ* sensor system. Moreover, due to the small volume

of the ADM the sensor response time is <1 s. Implementation of novel digital electronics is planned in order to replace the current analog QCL driver and CEU. The completed sensor will be installed in a mobile monitoring van operated by a University of Houston Earth and Atmospheric Sciences Center group and deployed for further real time measurements of CH_4 and N_2O emissions in the Greater Houston area in 2014.

Acknowledgements

The authors acknowledge financial support from a National Science Foundation (NSF) grant EEC-0540832 entitled "Mid-Infrared Technologies for Health and the Environment (MIRTHE)". The Rice University Laser Science group also acknowledges financial support from an NSF-ANR award for international collaboration in chemistry "Next generation of Compact Infrared Laser based Sensor for environmental monitoring (NexCILAS)" and a grant C-0586 for "Application of Mid-Infrared Quantum Cascade and Diode Lasers to High-Precision Atmospheric Trace Gas Monitoring" from the Robert Welch Foundation.

Notes and references

1 I. Mappé, L. Joly, G. Durry, X. Thomas, T. Decarpenterie, J. Cousin, N. Dumelie, E. Roth, A. Chakir and P. G. Grillon, *Rev. Sci. Instrum.*, 2013, **84**, 02103–02111.
2 I. Mappe-Fogaing, L. Joly, G. Durry, N. Dumelié, T. Decarpenterie and J. Cousin, *Appl. Phys. B: Lasers Opt.*, 2012, **108**, 933–943.
3 E. W. Wolff, *Philos. Trans. R. Soc., A*, 2011, **369**, 2133–2147.
4 J. Shen, T. J. Algeo, Q. L. Feng, L. Zhou, L. P. Feng, N. Zhang and J. H. Huang, *J. Asian Earth Sci.*, 2013, **75**, 95–109.
5 M. U. F. Kirschbaum, S. Saggar, K. R. Tate, K. P. Thakur and D. L. Giltrap, *Sci. Total Environ.*, 2013, **465**, 314–324.
6 R. Juszczak and J. Augustin, *Wetlands*, 2013, **33**(5), 895–907.
7 M. Austin, The Acad. of Dent. Learn. & OSHA Train., 2012, pp. 21–24.
8 O. Thomas, Oxford Instruments Plasma Technology, 2011, http://www.oxford-instruments.com.
9 *Guideline on Use of Nitrous Oxide for Pediatric Dental Patients*, American Academy of Pediatric Dentistry, 2009, vol. 33, pp. 190–193.
10 T. Risby and F. Tittel, *SPIE Optical Engineering*, 2010, **49**, 111123-1.
11 N. Tiliakos, J. S. Tyll, R. Herdy, D. Sharp, M. Moser and N. Smith, *AIAA Pap.*, 2001, 2001–3258.
12 V. Zakirov, M. Sweeting, T. Lawrence and J. Sellers, *Acta Astronaut.*, 2001, **48**(5), 353–362.
13 P. C. Castillo, I. Sydoryk, B. Gross and F. Moshary, *Proc. SPIE*, 2013, **8718**, J-1–J-12.
14 J. J. Scherer, J. B. Paul, H. J. Jost and M. L. Fischer, *Appl. Phys. B: Lasers Opt.*, 2013, **110**, 271–277.
15 J. Wojtas, Z. Bielecki, T. Stacewicz, J. Mikolajczyk, B. Rutecka and R. Medrzycki, *Acta Phys. Pol., A*, 2013, **124**, 592–594.
16 J. P. Lima, H. Vargas, A. Miklós, M. Angelmahr and P. Hess, *Appl. Phys. B: Lasers Opt.*, 2006, **85**, 279–284.
17 A. A. Kostrerev, Y. A. Bakhirkin, R. F. Curl and F. K. Tittel, *Opt. Lett.*, 2002, **27**, 1902–1904.
18 M. Jahjah, A. Vicet and Y. Rouillard, *Appl. Phys. B: Lasers Opt.*, 2012, **106**, 483–489.
19 R. Lewicki, G. Wysocki, A. A. Kosterev and F. K. Tittel, *Appl. Phys. B: Lasers Opt.*, 2007, **87**, 157–162.
20 N. Petra, J. Zweck, A. A. Kosterev, S. E. Minkoff and D. Thomazy, *Appl. Phys. B: Lasers Opt.*, 2009, **94**, 673–680.
21 L. Dong, J. Wright, B. Peters, B. A. Ferguson, F. K. Tittel and S. McWhorter, *Appl. Phys. B: Lasers Opt.*, 2012, **107**, 459–467.
22 J. Faist, *Quantum Cascade Lasers*, Oxford University Press, USA, 2013.
23 C. Gmachl, F. Capasso, D. L. Sivco and A. Y. Cho, *Rep. Prog. Phys.*, 2001, **64**, 1533–1601.
24 F. K. Tittel, L. Dong, R. Lewicki, G. Lee, A. Peralta and V. Spagnolo, nanophotonic devices IX, *Proc. SPIE*, 2012, **8268**, 82680F.
25 L. Dong, R. Lewicki, K. Liu, P. R. Buerki, M. J. Weida and F. K. Tittel, *Appl. Phys. B: Lasers Opt.*, 2012, **107**, 275–283.
26 F. Xie, C. Caneau, H. P. LeBlnc, N. J. Visovsky, S. Coleman, L. C. Hughes and C. Zah, *IEEE J. Sel. Top. Quantum Electron.*, 2012, **18**(5), 1605–1612.
27 L. Dong, A. A. Kosterev, D. Thomazy and F. K. Tittel, *Appl. Phys. B: Lasers Opt.*, 2010, **100**, 627–635.
28 http://www.cfa.harvard.edu/hitran/.
29 L. Dong, J. Wright, B. Peters, B. A. Ferguson, F. K. Tittel and S. McWhorter, *Appl. Phys. B: Lasers Opt.*, 2012, **107**, 459–467.
30 F. K. Tittel, L. Dong, R. Lewicki, G. Lee, A. Peralta and V. Spagnolo, *Proc. SPIE*, 2012, **8268**, 82680F–82681F.
31 F. K. Tittel, R. Lewicki, M. Jahjah, B. Foxworth and Y. Ma, *NATO Science for Peace and Security Series*, Springer, 2013.
32 M. Razeghi, L. Esaki and K. von Klitzing, Chapter 23, *Current Status of Mid-Infrared Semiconductor-Laser-based Sensor Technologies for Trace-Gas Sensing Applications* in *The Wonder of Nanotechnology: Quantum Optoelectronic Devices and Applications*, SPIE Press, Bellingham, WA, 2013, pp. 597–632.